Toxicology Letters 281 (2017) 44–52

Contents lists available at ScienceDirect

Toxicology Letters

journal homepage: www.elsevier.com/locate/toxlet

Full length article

Toxicology studies of primycin-sulphate using a three-dimensional (3D) *in vitro* human liver aggregate model

Ágota Pénzes[a], Elhusseiny Mohamed Mahmud Abdelwahab[b,c], Judit Rapp[b,c,d], Zsanett A. Péteri[a], Judit Bovári-Biri[a], Csaba Fekete[c,e], György Miskei[b,c], Krisztián Kvell[b,c], Judit E. Pongrácz[b,c,d,*]

[a] PannonPharma Ltd., Biological Control Laboratory, 1 Pannonpharma Str., H-7720, Pécsvárad, Hungary
[b] Department of Pharmaceutical Biotechnology, School of Pharmacy, University of Pécs, 2 Rókus Str., H-7624 Pécs, Hungary
[c] Szentágothai Research Center, University of Pécs, 20 Ifjúság Str., H-7624 Pécs, Hungary
[d] Humeltis Ltd, 20 Ifjúság Str., Pécs, Hungary
[e] Department of General and Environmental Microbiology, Faculty of Natural Sciences, University of Pécs, 6 Ifjúság Str., H-7624, Pécs, Hungary

ARTICLE INFO

Keywords:
Primycin-sulphate
Cytotoxicity
in vitro three-dimensional human liver model

ABSTRACT

Primycin-sulphate is a highly effective compound against Gram (G) positive bacteria. It has a potentially synergistic effect with vancomycin and statins which makes primycin-sulphate a potentially very effective preparation. Primycin-sulphate is currently used exclusively in topical preparations. *In vitro* animal hepatocyte and neuromuscular junction studies (in mice, rats, snakes, frogs) as well as in *in vitro* human red blood cell experiments were used to test toxicity. During these studies, the use of primycin-sulphate resulted in reduced cellular membrane integrity and modified ion channel activity. Additionally, parenteral administration of primycin-sulphate to mice, dogs, cats, rabbits and guinea pigs indicated high level of acute toxicity.

The objective of this study was to reveal the cytotoxic and gene expression modifying effects of primycin-sulphate in a human system using an *in vitro*, three dimensional (3D) human hepatic model system.

Within the 3D model, primycin-sulphate presented no acute cytotoxicity at concentrations 1 μg/ml and below. However, even at low concentrations, primycin-sulphate affected gene expressions by up-regulating inflammatory cytokines (*e.g.*, IL6), chemokines (*e.g.*, CXCL5) and by down-regulating molecules of the lipid metabolism (*e.g.*, peroxisome proliferator receptor (PPAR) alpha, gamma, etc). Down-regulation of PPAR alpha cannot just disrupt lipid production but can also affect cytochrome P450 metabolic enzyme (CYP) 3A4 expression, highlighting the need for extensive drug–drug interaction (DDI) studies before human oral or parenteral preparations can be developed.

1. Introduction

Antibiotics are amongst the most frequently used medications in modern medicine. Today, over one hundred different antibiotics are available to cure minor discomforts as well as life-threatening infections. The overuse of broad-spectrum antibiotics has recently resulted in an alarming number of human pathogens that acquired resistance genes making most available antibiotics ineffective in therapy. For the above reasons, development of new preparations is essential.

Dating back to 1954 (Valyi-Nagy et al., 1954), a novel drug named primycin was discovered with great antimicrobial potential that had different chemical and biological properties from all known antibiotics. Primycin is a thermostable, poorly water soluble, absorptive, surface-active non-polyene macrolide lactone antibiotic complex that exhibits a broad antimicrobial spectrum (Valyi-Nagy et al., 1954). The individual compounds all exert antimicrobial activity and act synergistically making primycin a powerful antibiotic effective against both Gram (G) positive and G negative bacterial strains (Nógrádi, 1988; Uri and Actor, 1979; Uri, 1986). For a long time, no primycin resistance was observed identifying primycin as an antibiotic with great potential. However, application of other macrolide antibiotics (*e.g.*, vancomycin, mupirocin) has slightly changed the original observation. Although the bactericidal effect of primycin-sulphate is concentration dependent, it is still effective against all examined G positive bacteria (Feiszt et al., 2014). Even against MRSA isolates, primycin-sulphate showed slightly higher activity than mupirocin, and inhibited the growths of mupirocin-resistant strains (Feiszt et al., 2014). Additionally, while spontaneous resistance did not occur against primycin-sulphate, serial passages achieved such

* Corresponding author at: Department of Pharmaceutical Biotechnology, School of Pharmacy, and Szentagothai Research Centre, University of Pecs, 2 Rokus Str, Pecs, H-7624, Hungary.
E-mail address: pongracz.e.judit@pte.h (J.E. Pongrácz).

http://dx.doi.org/10.1016/j.toxlet.2017.09.005
Received 31 May 2017; Received in revised form 9 September 2017; Accepted 11 September 2017
Available online 13 September 2017
0378-4274/

resistance (Feiszt et al., 2014). Bacterial strains demonstrating elevated minimal inhibitory concentrations (MIC) for primycin-sulphate have also shown increased MIC values for vancomycin and daptomycin although the mechanism has not yet been investigated further (Feiszt et al., 2014). While earlier studies have identified primycin-sulphate as a drug against polyresistant G negative bacterial strains as well as some pathogenic yeasts and filamentous fungi (Nógrádi, 1988; Uri and Actor, 1979; Uri, 1986), recent experiments have found primycin-sulphate non-effective against G negative bacteria in topical applications (Feiszt et al., 2014). Other studies have also shown that in lower concentrations, primycin-sulphate facilitates substance permeability of vesicles formed by G positive bacteria but did not affect ones formed by G negative bacteria (Adám-Vizi et al., 1980). Nevertheless, further investigations were recommended for topical applications due to effectiveness of primycin-sulphate against multiresistant G positive pathogens (Feiszt et al., 2014). Topical preparation of primycin-sulphate already exists in the form of the Ebrimycin® gel for prevention of burn infections, bacterially infected trophic ulcers, post-operative suppurations, inflammation of the anorectum, etc (Bálint, 1987; Bíró and Várkonyi, 1987; Mészáros et al., 1979; Papp et al., 1990). Since primycin-sulphate is absorbed at a very slow rate from excoriated areas and mucous membranes we theorized that low doses of primycin-sulphate (Nógrádi, 1988; Uri and Actor, 1979; Valyi-Nagy and Kelentey, 1960) might be applicable to effectively treat human infections using an oral or parenteral preparation of the drug.

The theory, however, requires further investigation as primycin-sulphate was highly toxic when administered parenterally in various animal species (mice, dogs, cats, rabbits and guinea pigs) (Nógrádi, 1988; Uri and Actor, 1979; Valyi-Nagy and Kelentey, 1960). In contrast, when oral applications were tested in cats, dogs and guinea pigs (Nógrádi, 1988; Uri and Actor, 1979; Valyi-Nagy and Kelentey, 1960), primycin-sulphate did not induce acute toxic reactions leaving open the possibility for further drug development. However, how human tissues would be affected by primycin-sulphate the knowledge was limited to red blood cells, where membrane integrity was lost when treated with the drug (Blasko et al., 1986). In rat hepatocytes, membranes of mitochondria and nuclei were also affected (Mészáros et al., 1979). Studies using bacteria and yeast have revealed that primycin-sulphate can disorganize their cell membranes, resulting in a dose-dependent increase of ion permeability and conductivity (Feiszt et al., 2017; Horváth et al., 1979) causing structural changes to yeast membranes, resulting in disrupted membrane potential (Virag et al., 2010; Virág et al., 2012).

In the present work, effects of primycin-sulphate was evaluated in an *in vitro* three-dimensional (3D) human liver tissue aggregate model system that mimics *in vitro* the structure and function of the human liver. Our studies investigated primycin-sulphate induced gene expression changes by orally non-toxic (Valyi-Nagy and Kelentey, 1960) but effective antibacterial concentrations of the drug (Feiszt et al., 2014). Special attention was given to genes affecting the lipid metabolism as in previous reports loss of both cellular and mitochondrial membrane integrity have been demonstrated.

2. Materials and methods

2.1. Cell cultures

Human hepatocellular liver carcinoma cell line (HepG2) was purchased from ATCC (LGC Standards GmbH) and were cultured in DMEM supplemented with 10% fetal calf serum (FCS) (Lonza). Cell cultures were maintained in 5% CO_2 at 37 °C in a humidified atmosphere and passaged at 80% confluency. Primary human hepatocytes (hNHEPS) were purchased from Lonza. The seeding density for attachment was approximately 150000 cells/cm^2. hNHEPS were cultured in hepatocyte culture medium (HBM Hepatocyte Basal Medium, Lonza) supplemented with a cocktail of growth factors and hormones (Lonza), gentamycin (10 µg/ml), amphotericin B (2.5 ng/ml) and 2% bovine serum albumin (BSA) (Lonza) using plates coated with Type I Collagen (BD). Cell cultures were maintained in 5% CO_2 at 37 °C in a humidified atmosphere and the growth medium was changed three hours after seeding and every day thereafter. Primary human fibroblast (Fb) were purchased from Lonza and cultured in fibroblast culture medium (FBM Fibroblast Growth Medium) (Lonza) supplemented with a mixture of growth factors and hormones (Lonza), gentamycin (10 µg/ml), amphotericin B (2.5 ng/ml) and 2% FCS. The seeding density for attachment was approximately 2500 cells/cm^2. Cell cultures were maintained in 10% CO_2 at 37 °C in a humidified atmosphere and passaged at 80% confluency. Medium was changed the day after seeding and every other day thereafter.

Table 1
Models.

	Cell number (cells/well)	HepG2/Hepatocyte cell ratio	Fibroblast cell ratio
2D HepG2 monoculture	10^4	100%	–
3D HepG2 monoculture	10^5	100%	–
2D Fb monoculture	10^4	–	100%
3D Fb monoculture	10^5	–	100%
2D HepG2: Fb co-culture	10^4	20%	80%
3D HepG2: Fb co-culture	10^5	20%	80%
3D hNHEPS: Fb co-culture	10^5	20%	80%

2.2. Models

Seven different types of *in vitro* tissue models were set up, summarized in Table 1: two-dimensional (2D) and three-dimensional (3D) HepG2 mono-cultures, 2D and 3D Fb mono-cultures, HepG2 and Fb co-cultures and 3D hNHEPS and Fb co-cultures. For 2D cell cultures, 10^4 cells/wells were used and the hepatocyte to fibroblast ratio in co-cultures was 1:4. 3D cell cultures were set up in V-bottom-well plates using 10^5cells/well. The hepatocyte to fibroblast ratio in co-culture models was 1:4. Cells were pelleted in 96 well, V-bottom plates for 5 min at 1500 rpm. The 2D and 3D cultures were maintained in 5% CO_2 at 37 °C in a humidified atmosphere. The 3D aggregates formed within 24 h. Known hepatocyte differentiation markers (*e.g.*, albumin (Hu et al., 1992), KRT19 (Gumerova et al., 2007; Malinen et al., 2014), CYP3A4 (Thomas et al., 2005)) were tested by gene expression analysis for quality control of each tissue batch (Fig. S1A, S1B, S1C and S1D).

2.3. Chemicals

Primycin-sulphate (MW = 1127.25, average mass) was provided by the manufacturer (PannonPharma Ltd.). The content of active agent was 865.03 U mg^{-1}.

2.4. Treatments

Cell cultures were treated with 0.1; 1.0; 10; 100 µg/ml primycin-sulphate −dissolved in DMSO- for 72 h. Control cultures were incubated in the presence of DMSO and chloropromazine.

For testing the effect of primycin-sulphate on lipid metabolism, HepG2 and Fb 3D co-cultures were also treated with 0.2 µg/ml and 2 µg/ml, prednisolone for 72 h as a positive control for PPAR activation. After treatment, the aggregates were collected into RA1 lysis buffer solution for RNA isolation and into cryomolds for dissection.

2.5. Histology

3D HepG2 and Fb co-cultures were fixed in 4% formalin for 30 min, and after embedding in PolyFreeze (Polysciences, Inc.) tissue freezing medium, tissues were frozen at −70 °C. 9 μm thick cryostat sections were placed on poly-L-lysine coated glass slides and stained with hematoxylin using standard techniques. The sections were analyzed and pictures were taken with 10×, 20× and 40× objectives using an Olympus BX61 microscope equipped with a CCD camera and AnalySIS software.

2.6. RNA isolation, preparation of cDNA

For testing hepatocyte differentiation marker gene expressions, total RNA was isolated from the various cultures using EZ-10 Spin Column Total RNA Minipreps Super kit (Bio Basic Inc.), following the manufacturer's instructions. Following RNA isolation, DNAse digestion was performed using a DNAse digestion kit (Fermentas). RNA concentrations were quantified with Qubit (Invitrogen). cDNA was constructed using the High Capacity RNA to cDNA kit according to the manufacturer's instructions (Applied Biosystems). For PPAR gene expression investigation RNA isolation was performed using NucleoSpin® RNA kit (Macherey-Nagel) according to the manufacturer's instructions. RNA concentration was measured using Eppendorf BioSpectrometer Basic (Eppendorf). cDNA synthesis was performed using High-Capacity cDNA Reverse Transcription Kit (Applied Biosystems, Life Technologies).

2.7. Microarray analysis

Microarray hybridisations of mRNA samples were performed using the Affymetrix GeneAtlas System and Human Genome U 219 Array chip (Affymetrix) to analyze the expression level of 20,000 genes and more than 36,000 transcript variants. 2D, 3D mono- and co-cultures were prepared as described earlier, and were treated or untreated with 1 μg/ml primycin-sulphate for 48 h. The samples were then prepared according to the manufacturer's instructions (Affymetrix). Total RNA was isolated using EZ-10 Spin Column Total RNA Minipreps Super kit as recommended by the manufacturer (Bio Basic Inc.). Quality of RNA was assessed by Agilent 2100 bioanalyser using the RNA 6000 Nano Chip (Agilent Technologies), and quantity was determined by Nanodrop-2000 Spectrophotometer (Thermo Scientific). The protocol (reverse transcription, labeling, fragmentation and hybridisation) was performed according to the manufacturer's instructions (Affymetrix). The raw intensity files (CEL) were generated by the Affymetrix GeneAtlas Instrument Control Software (Affymetrix). The intensity values of CEL files were normalized to remove bias between the arrays, using the Robust Multi-array Average (RMA) algorithm. The microarray data analysis was performed by Astrid Research Ltd (Astrid Research Ltd.). Study composition is shown in Fig. S1E.

2.8. Quantitative (q)RT-PCR analysis

Real-time qRT-PCR analysis of the differentiation marker genes was performed using ABI 7900HT Real-Time PCR system, ABI Prism 7900 Sequence Detection System Software system and ABI Power SYBR green PCR master mix. For PPAR gene expression analysis ABI StepOnePlus Real-Time PCR system and SensiFast Sybr High-Rox mix (BioLine) was used. Thermal cycling consisted of an UNG activation step for 2 min at 50 °C and an initial denaturation step for 10 min at 95 °C followed by 40 cycles of denaturation and annealing/extension. Expression levels were estimated using the ΔΔCt method and normalized to beta-actin. ΔΔCt was transformed into fold-change using the following formula: fold change = 2. The primer sequences are listed in Table 2.

2.9. Hepatocyte ureagenesis activity assay

The urea concentration was determined using QuantiChrom™ Urea Assay Kit (DIUR-500, BioAssay Systems). 2D and 3D HepG2 monoculture and HepG2 and Fb co-culture models were cultivated for 1, 3 and 5 days. The culture medium samples were assayed directly in a clear bottom 96-well plate in duplicates. Optical density was measured at 430 nm after 50 min incubation at room temperature and urea concentration (mg/dL) of the samples were calculated according to manufacturer's instructions (BioAssay Systems). The absorbance was measured with a MultiScan Ascent microplate reader (Thermo Labsystems).

2.10. End point viability assay

2.10.1. Colorimetric assay (MTT-assay)

Experimental evaluation of primycin-sulphate toxicity was tested in primary human hepatocyte and HepG2-primary human fibroblast co-cultures using the MTT (3-(4,5-Dimethylthiazol-2-yl)-2,5-diphenyltetrazolium bromide, a tetrazole) (Sigma–Aldrich Co.) assay. In the current literature there are no recommended concentrations for in vitro studies of primycin-sulphate, therefore based on the results of *in vivo* experiments, various concentrations (100 μg/ml, 10 μg/ml, 1.0 μg/ml, 0.1 μg/ml final concentrations) of the drug were tested. Microplates were incubated for 72 h in 5% CO_2 humidified atmosphere at 37 °C prior to the assay. MTT was dissolved in phenol-red free DMEM (Lonza) and the precipitate was solubilized in a mixture of dimethyl sulfoxide and isopropanol (VWR Prolabo) (1:1). The absorbance of the colored solution was quantified by absorbance using Multiskan Ascent ELISA plate reader at 450 nm (Thermo Fisher Scientific Inc.). Treatment set-up is summarized in Table S1.

2.10.2. Luminescent assay

Primycin-sulphate (0.1 μg/ml and 1.0 μg/ml final concentration) and prednisolone (0.2 μg/ml and 2.0 μg/ml final concentration) toxicity was tested in monolayer HepG2-primary human fibroblast co-cultures using CellTiter-Glo Luminescent Cell Viability Assay (Promega) and in three-dimensional co-cultures using CellTiter-Glo 3D Cell Viability Assay (Promega). Microplates were incubated for 24 and 48 h in 5% CO_2 humidified atmosphere at 37 °C. Cell viability was measured following the manufacturer's instructions using Synergy HT Multi-Mode Microplate Reader (BioTek Instruments). Treatment set-up is summarized in Table S1.

2.11. Lipidtox staining

Sections of 3D HepG2:Fb co-cultures grown on 4 chamber culture slides (BD Falcon™) were fixed in 4% PFA for 20 min, then gently rinsed with PBS. The HSC LipidTOX™ Red neutral lipid stain (Invitrogen) was applied to the slides in 1:1000 dilution for 30 min. Pictures were taken with ZeissLSM 710 confocal microscope.

2.12. PPAR gamma reporter assay

HepG2 cells were seeded on 6-well plates in 10^5/well density. After 24 h fresh media was provided to the attached cells and transfection with PPRE plasmid was performed using PEI (Sigma). We thank Dr. R. M. Evans (The Salk Institute for Biological Studies, La Jolla, CA, USA) for the PPRE-TK-luciferase reporter construct. After 5 h of transfection, fresh media was applied to the cells that were maintained for 72 h when they were treated with prednisolone (2.0 μg/ml final concentration) and with primycin-sulphate (1.0 μg/ml and 0.1 μg/ml final concentration) for another 72 h, respectively. Following incubation, the media was removed and the cells were lysed in PBS containing 0.1% TritonX. PPAR gamma activity was measured on Synergy™ HT Plate Reader (BioTek Instruments) using luciferase activity assay.

Table 2
Primer sequences.

GENES	ABBREVIATIONS	PRIMER SEQUENCES
Human albumin.	ALB	5′-GATGTCTTCCTGGGCATGTT-3′ 5′-AGCAGCAGCACGACAGAGTA-3′
Human alpha-fetoprotein	AFP	5′-CTTGTGAAGCAAAAGCCACA-3′ 5′-CCCTCTTCAGCAAAGCAGAC-3′
Human keratin 18, transcript variant 1	KRT18	5′-CACAGTCTGCTGAGGTTGGA-3′ 5′-CAAGCTGGCCTTCAGATTTC-3
Human keratin 19	KRT19	5′-TGAGCAGGTCCGAGGTTACT-3′ 5′- TCTTCCAAGGCAGCTTTCAT-3′
Human cytochrome P450, family 3, subfamily A, polypeptide 4	CYP3A4	5′- TTCAGCAAGAAGAACAAGGACAA −3′ 5′- GGTTGAAGAAGTCCTCCTAAGC −3′
Human glyceraldehyde-3-phosphate dehydrogenase	GHDP	5′-AAATCAAGTGGGGCGATGCTG-3′ 5′-GCAGAGATGATGACCCTTTTG-3′
Human adipose differentiation-related protein	ADRP	5′-CCGTCGATTTCTTTCTCCAG-3′ 5′-TGATGGTCTTCACACCGTTC-3′
Human peroxisome proliferator-activated receptor alpha	PPARA	5′-GTAGAATCTGCGGGGACAAG-3′ 5′- GTTGTGTGACATCCCGACAG-3′
Human peroxisome proliferator-activated receptor gamma	PPARG	5′- GCTTTTGGCATACTCTGTGATCTC −3′ 5′- GGTGGCCATCCGCATCT −3′
Human beta-actin	ACTB	5′- GCGCGGCTACAGCTTCA −3′ 5′- CTTAATGTCACGCACGATTTCC −3′

2.13. Statistics

All results are presented as mean of standard error shown as error bars. The effect of treatments was analyzed statistically by Student's *t*-test. Calculations were performed with the SPSS statistical software. A value of $P < 0.05$ was considered to be statistically significant (*).

3. Results

To investigate the toxic effects of primycin-sulphate on the human liver, liver-like *in vitro* liver tissue models were set up using primary human hepatocytes and fibroblasts as recommended by previous studies (Bhatia et al., 1999; Khetani and Bhatia, 2008; Breslin and O'Driscoll, 2013; Bell et al., 2016). As hepatocytes lose their tissue specific characteristics over time in 2D culture, 3D culture conditions were characterized (Fig. S1). Gene expression and functionality tests revealed that characteristic liver function markers (*e.g.* KRT18, etc.) (Chougule and Sumitran-Holgersson, 2012) are expressed mainly by the 3D co-cultures (Fig. S1) making such in vitro models suitable for toxicity screening of primycin-sulphate.

3.1. Low doses of primycin-sulphate was non-toxic in acute toxicity tests

We examined the effect of primycin-sulphate using an MTT (Fig. 1.) and a luminescent viability test (Table S1), (Fig. S2) in various hepatic culture conditions. The 3D HepG2 monoculture model was not suitable to investigate the effects of primycin-sulphate, as within 24 h, primycin-sulphate had induced structural damage in such cultures. Similar damage was not detected in control cultures (data not shown). At higher concentrations of primycin-sulphate (10–100 µg/ml), 2D co-cultures were more sensitive to primycin-sulphate induced cell death than 3D co-cultures (Fig. 1). In contrast, lower concentration (0.1–1.0 µg/ml) of primycin-sulphate had no remarkable effect on cell viability in any culture conditions (Fig. 1). 3D HepG2:Fb and primary human hepatocyte:Fb co-culture models in toxicity assays had shown no significant difference compared to hepatocyte and HepG2 containing 3D monocultures (Fig. 1). Similarly, non-toxic effects of primycin-sulphate in low concentrations (1.0 µg/ml and 0.1 µg/ml final concentration) was confirmed by an independent method (Fig. S2) in which primycin-sulphate did not decrease ATP production in a luminescent assay, which is an accepted sign of maintained cellular viability.

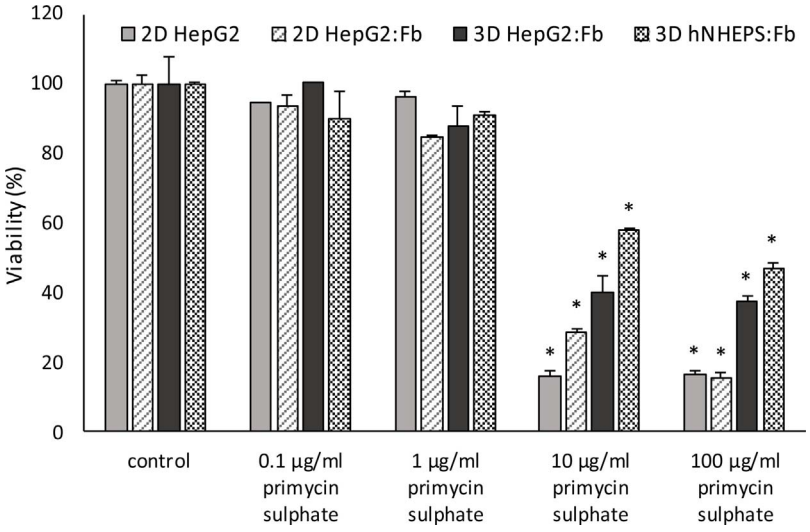

Fig. 1. Assessment of primycin-sulphate toxicity.
Assessment of primycin-sulphate induced changes in cellular viability using 2D HepG2, HepG2-fibroblast co-culture; 3D HepG2 and fibroblast as well as primary human hepatocyte and fibroblast co-culture models. Cells were treated with different doses of primycin-sulphate for 72 h and viability was compared to medium control. The cell proliferation was assessed by methylthiazolium (MTT) assay. Statistically significant changes were marked by an asterisk (*). At concentrations 10 and 100 µg/ml viability was significantly ($p = 0.001$) reduced in all model cultures.

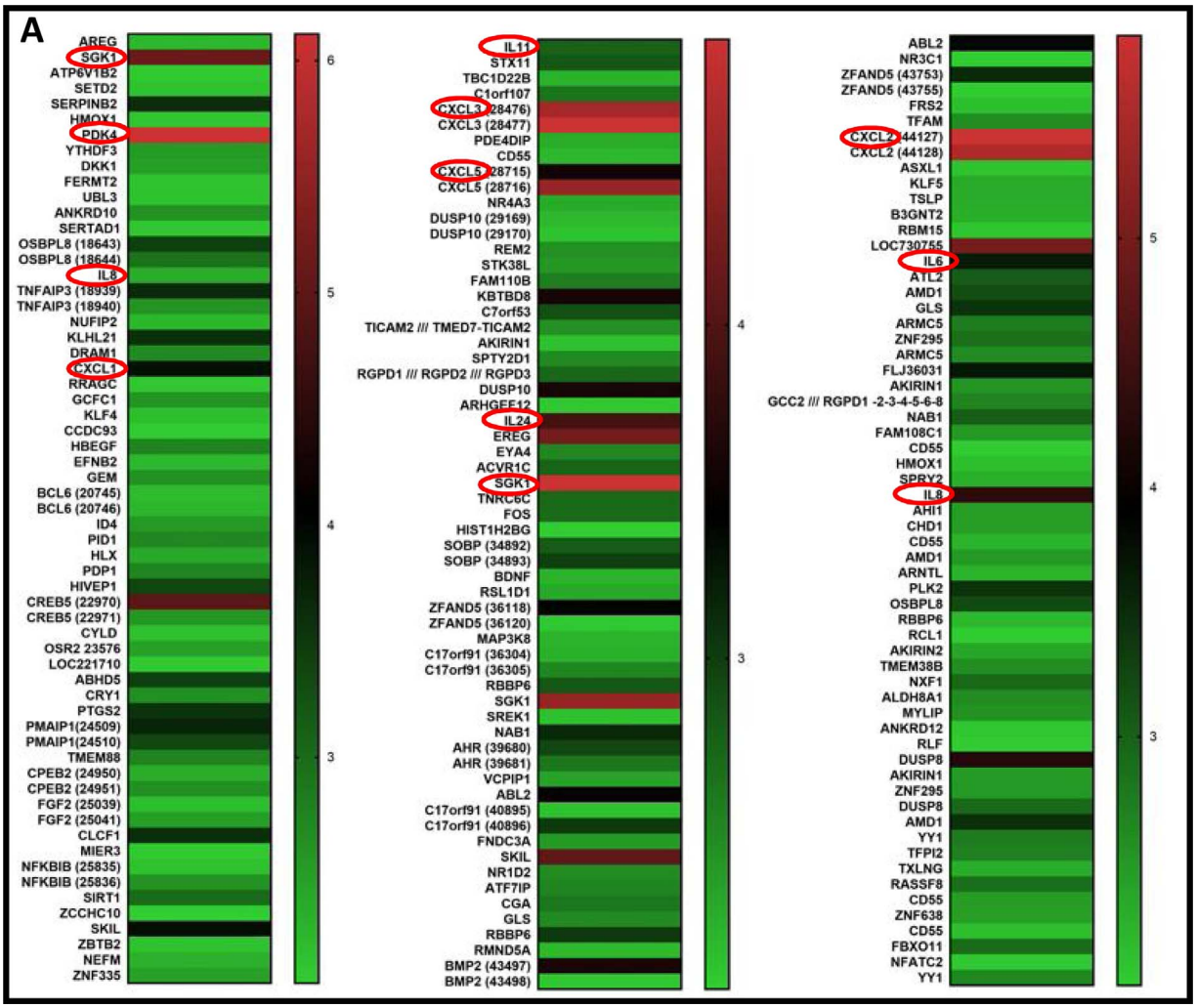

Fig. 2. Affymetrix array analysis of gene expression changes after primycin-sulphate treatment of 3D HepG2-fibroblast co-cultures (n = 5).

A. Heat-map representation of gene expression up-regulation after 1.0 μg/ml primycin-sulphate treatment by 48 h. Data is presented as fold change against control 3D HepG2-fibroblast co-cultures.

B. Heat-map representation of gene expression down-regulation after 1.0 μg/ml primycin-sulphate treatment for 48 h. Data is presented as fold change against control 3D HepG2-fibroblast co-cultures.

C. Cytokine and chemokine gene expression changes triggered by 1.0 μg/ml primycin-sulphate treatment and in untreated control 3D HepG2-fibroblast co-culture aggregates are presented by the graph. Expression increase or decrease was compared to untreated 2D HepG2-fibroblast co-cultures.

D. Up-regulated lipid metabolism associated gene expressions triggered by 1.0 μg/ml primycin-sulphate treatment and in untreated control 3D HepG2-fibroblast co-culture aggregates are presented by the graph. Expression increase or decrease was compared to untreated 2D HepG2-fibroblast co-cultures.

E. Down-regulated lipid metabolism associated gene expressions triggered by 1.0 μg/ml primycin-sulphate treatment and in untreated control 3D HepG2-fibroblast co-culture aggregates are presented by the graph. Expression increase or decrease was compared to untreated 2D HepG2-fibroblast co-cultures.

3.2. Affimetrix gene expression array analysis revealed the effects of primycin-sulphate on inflammatory and lipid metabolism

Hybridisations of mRNA-s isolated from 3D HepG2:Fb control and primycin-sulphate treated samples to the Affymetrix microarray revealed that by 28 h, out of 20,000 genes and more than 36,000 transcript variants at cut-off 2, 184 genes were up- (Fig. 2A) and 259 were down-regulated upon 1 μg/ml primycin-sulphate treatment. (Fig. 2B). To emphasize gene expression changes triggered by primycin-sulphate and not by the modification of cell culture conditions, gene transcript levels measured in 3D HepG2:Fb co-cultures aggregates controls or primycin-sulphate treated (1.0 μg/ml) were compared to 2D HepG2:Fb co-cultures (Fig. 2C–E). The most robustly up-regulated genes included inflammatory cytokine genes IL6 (3.6-fold), IL8 (2.3-fold), IL11 a member of the IL-6 family (2.7-fold) and IL24 an IL10 interleukin family member (3.9-fold). Several chemokine genes (CXCL5, −3, −2, −1) were also increased (4.4-, 4.8-, 5.5, 3.8-fold, respectively) (Fig. 2C). Additionally, 1 μg/ml primycin-sulphate treatment also resulted in a 6-fold increase in Pyruvate Dehydrogenase Kinase 4 (PDK4), an important enzyme in lipid metabolism, a 5-fold increase in serum/glucocorticoid regulated kinase 1 (SGK1) – a regulator of glucose and lipid metabolism, and a 3-fold increase in sirtuin 1 (SIRT1) expression (Fig. 2C). Meanwhile, other lipid metabolism associated genes (*e.g.* apolipoprotein B (APOB), Mediator Complex Subunit 20 (MED20), Cytochrome C Oxidase Assembly Factor 1 Homolog (C7orf44) and Fatty Acid- Binding Protein 1 (FABP1)) decreased substantially (3.2-, 3.2-, 3.2-, 3-fold, respectively) (Fig. 2E).

3.3. Non-toxic concentrations of primycin-sulphate modulate PPAR gene expression and activity

Acute cytotoxicity studies (Fig. 1 and Fig. S2) have shown that there are potentially some concentrations of primycin-sulphate that although appear non-toxic to the human hepatic aggregate tissues, can still affect gene expressions (Fig. 2) associated with inflammation and the lipid metabolism. PDK4 for example is activated by long chain fatty acids

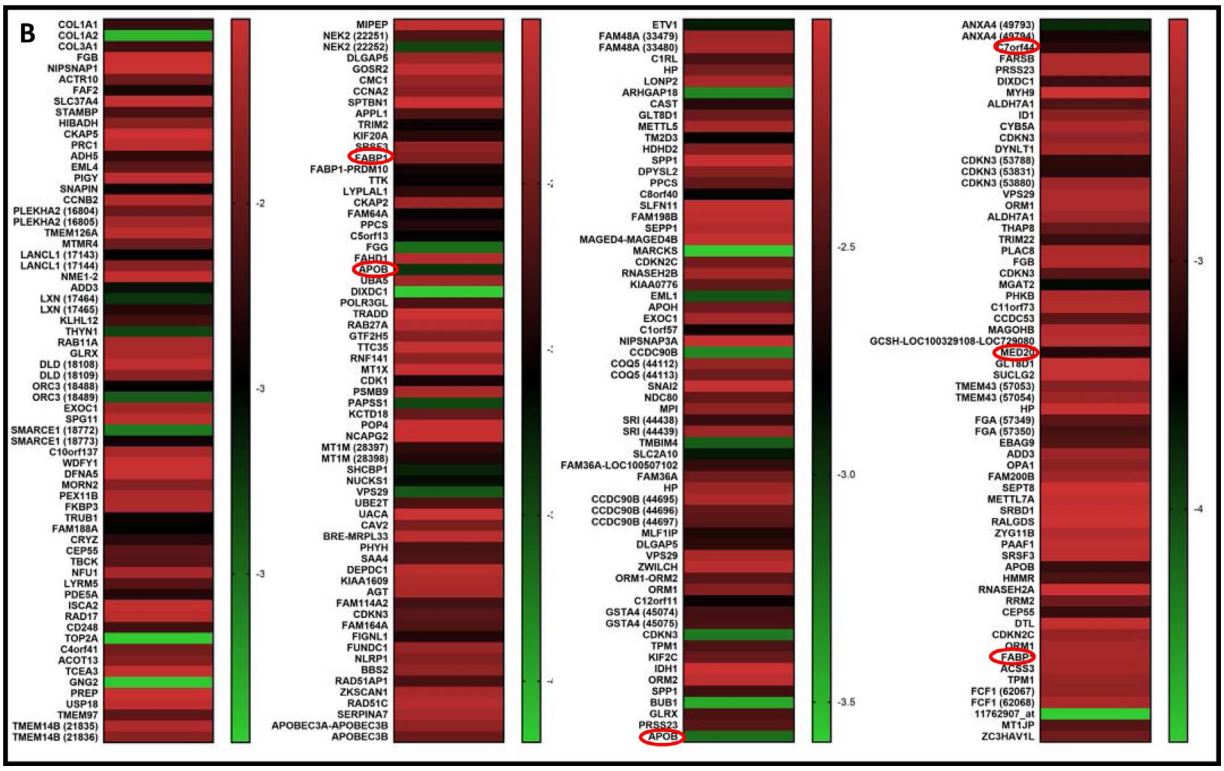

Fig. 2. (*continued*)

and pharmacologic ligands of PPAR alpha (Song et al., 2010), while SGK1 regulates adipocyte differentiation (Di Pietro et al., 2010), in close association with SIRT1 and PPAR gamma activity (Pirat et al., 2017). To test the effect of primycin-sulphate on the lipid metabolism regulator PPAR family, we used the non-toxic prednisolone, a known modulator of the PPARs, as positive control (Fig. S2). In our test systems prednisolone treatment induced PPAR alpha, PPAR gamma and their downstream target ADRP up-regulation at the mRNA (Fig. 3A) level by 24 h of treatment. Additionally, prednisolone induced high PPAR activity, measured by the PPAR reporter system (Fig. S3) indicating lipid

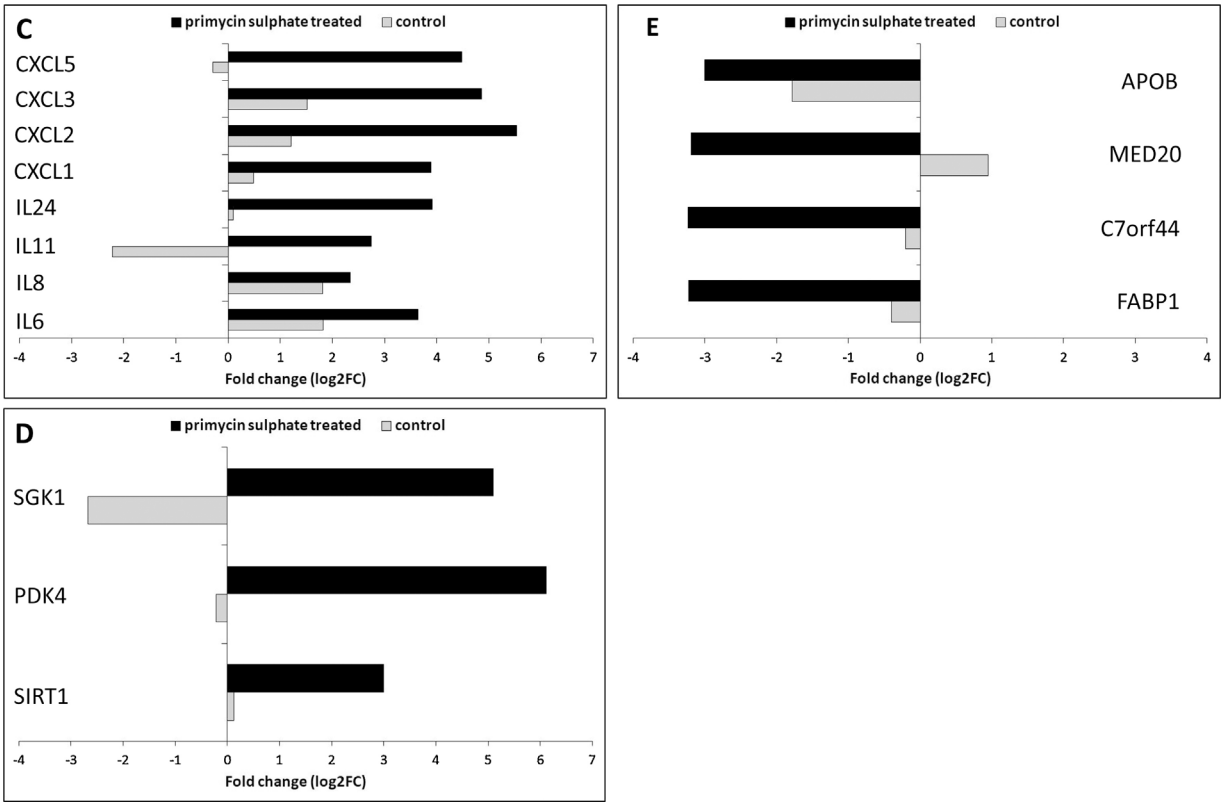

Fig. 2. (*continued*)

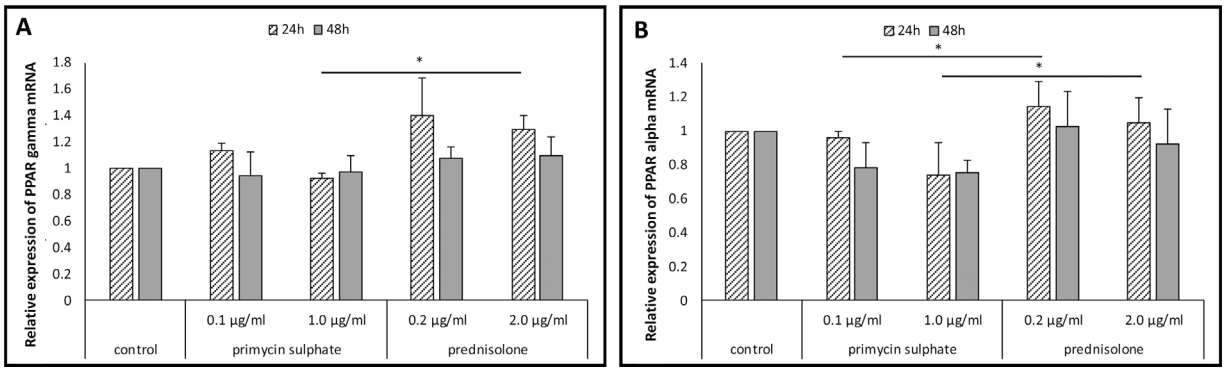

Fig. 3. PPAR activity and expression following primycin-sulphate treatment.
A. PPAR alpha mRNA levels were measured using qRT-PCR in 3D HepG2-fibroblast co-cultures after treatment with different doses of primycin-sulphate and prednisolone for 24 and 48 h. Data was analyzed by the ΔΔCt method where beta-actin was the reference gene. Data are expressed as fold change. Statistically significant changes were marked by an asterisk (*).
B. PPAR gamma mRNA levels were measured using qRT-PCR in 3D HepG2-fibroblast co-cultures after treatment with different doses of primycin-sulphate and prednisolone for 24 and 48 h. Data was analyzed by the ΔΔCt method where beta-actin was the reference gene. Data are expressed as fold change. Statistically significant changes were marked by an asterisk (*).
C. ADRP mRNA levels were measured using qRT-PCR in 3D HepG2-fibroblast co-cultures after treatment with different doses of primycin-sulphate and prednisolone for 24 and 48 h. Data was analyzed by the ΔΔCt method where beta-actin was the reference gene. Data are expressed as fold change. Statistically significant changes were marked by an asterisk (*).
D. Intracellular accumulation of neutral lipids. Intracellular accumulation of neutral lipids were detected using LipidTox Deep (red) reagent. While prednisolone increased lipid accumulation, primycin-sulphate reduced lipid accumulation even in areas of cellular membranes. A representative staining is shown (n = 3).

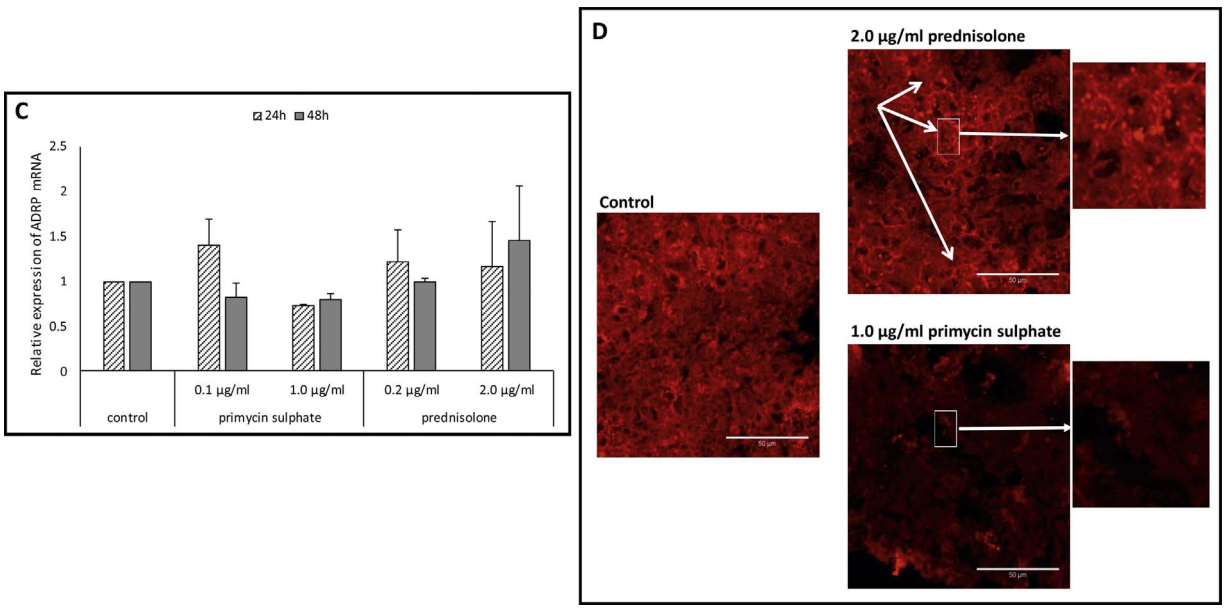

Fig. 3. (*continued*)

pathway activation. In contrast, primycin-sulphate triggered down-regulation of PPAR alpha, PPAR gamma and ADRP genes at both 0.1 and 1.0 g/ml concentrations by 24 h (Fig. 3A–C) that was further decreased by 48 h of incubation (Fig. 3A, 3 B and 3C). (In prednisolone treated samples PPAR alpha expression was significantly higher than in primycin-sulphate treated cultures at both concentrations ($p = 0.025$ and $p = 0.020$, respectively). PPAR gamma expression was significantly higher following 2.0 µg/ml prednisolone treatment ($p = 0.001$)). PPAR activation was also transient leading to decreased PPAR reporter activity by 48 h of treatment indicating interference with lipid metabolism (Fig. S3). In support of the above findings, prednisolone treatment lead to accumulation of lipid droplets in cells tested by lipidtox staining (Fig. 3D), while primycin-sulphate triggered down-regulation of cellular lipids even in the cellular membranes (Fig. 3D).

3.4. Primycin-sulphate down-regulates PPAR alpha target CYP3A4

As PPAR alpha is also a transcriptional regulator of CYP3A4, a prominent member of the CYP enzyme family and an important detoxification enzyme, CYP3A4 levels were tested both after prednisolone and primycin-sulphate treatment. While up-regulation of CYP3A4 mRNA levels was detected after prednisolone 0.2 and 2.0 µg/ml treatment (Fig. 4) ($p = 0.01$ and $p = 0.016$, respectively), 0.1 and 1.0 µg/ml primycin-sulphate significantly reduced CYP3A4 expression (Fig. 4) ($p = 0.001$, $p = 0.001$, respectively).

4. Conclusion

As the number of multi-resistant bacterial strains are on the rise, re-assessment of primycin-sulphate as a human antimicrobial oral or parenteral preparation appears highly appropriate.

Using an in vitro human, 3D liver tissue model provided the first glimpse of the effects primycin-sulphate might have on the human liver. Primycin-sulphate demonstrated a dose-dependent acute cytotoxicity pattern in all culture types at concentrations of 10 and 100 µg/ml. At lower concentrations that were still in the antimicrobial range (Valyi-Nagy and Kelentey, 1960), hepatocytes or HepG2 cells especially in 3D

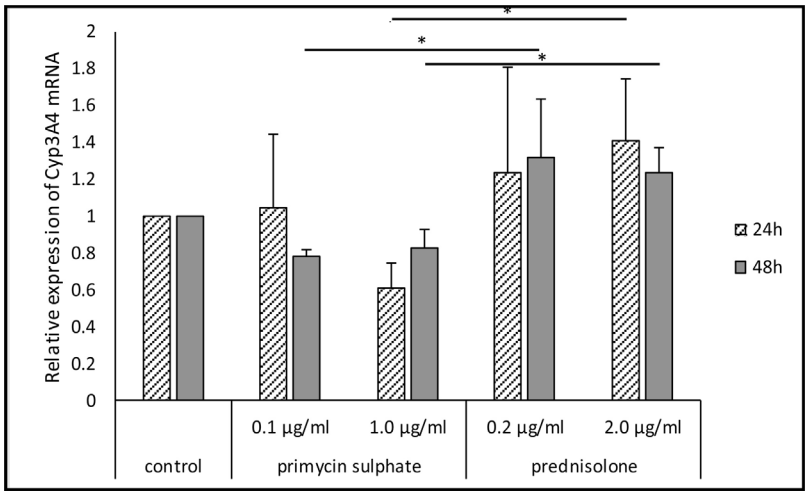

Fig. 4. Primycin-sulphate affects CYP3A4 transcription.
Expression of CYP3A4 in 3D HepG2-fibroblast co-cultures treated with different doses of primycin-sulphate and prednisolone for 24 and 48 h by QRT-PCR. Data was analyzed by the ΔΔCt method where beta-actin was the reference gene. Data are expressed as fold change. Statistically significant changes were marked by an asterisk (*).

co-cultures tolerated the drug. At "non-toxic" concentrations of primycin-sulphate (1.0 g/ml or lower) molecules regulating inflammation or the lipid metabolism were detected. IL11 and IL24 interleukin genes were even more strongly increased than the expression of inflammatory cytokine genes IL6 and IL8. As both IL11 (Johnstone et al., 2015) and IL24 (Manesh et al., 2015) have recently been connected to carcinogenesis and targets of anti-cancer therapy, such effects of primycin-sulphate should be noted in future drug development. Genes affecting the CXC subfamily of chemokines were also strongly up-regulated. Chemokines, which recruit and activate leukocytes, are classified by function (inflammatory or homeostatic) or by structure. The primycin-sulphate induced up-regulation of chemokines (CXCL-1, –2, –3, –4, –5) all belong to the same subfamily They bind to the G-protein coupled receptor chemokine (CXC motif) receptor 2 to recruit neutrophils in order to promote angiogenesis. But *e.g.*, CXCL-5 is also an adipokine by activating the Jak2/Stat5 pathway that inhibits insulin signaling and promotes obesity (Chavey and Fajas, 2009). Up-regulation of inflammatory cytokines IL6 and IL8 have also been linked to the lipid metabolism via the PPAR family (Straus and Glass, 2007). One of many functions of PPAR is inhibiting inflammatory actions such as cytokine and chemokine secretion when they are activated by endogenous or synthetic ligands. In contrast to the anti-inflammatory prednisolone, primycin-sulphate did not induce up-regulation of PPAR family members (Fig. 2F) but showed slight decreases in PPAR gene expression and their target – ADRP (Fig. 2G). Although reduction of PPAR family members were not significant compared to untreated controls, PPAR alpha levels and activity were reduced by both 0.1 and 1 µg/ml primycin-sulphate which lead to significant down-regulation of its target gene, CYP3A4 mRNA levels. Although there are several drugs that affect CYP3A4 activity including anti-HIV agents (Ernest et al., 2004; Sevrioukova and Poulos, 2010), antidepressants (DeVane et al., 2004), as well as some other macrolide antibiotics (*e.g.*, clarithromycin, and erythromycin) (Carls et al., 2014; Vermeer et al., 2016), neither drugs are inhibitors of CYP3A4 transcription, only activity (FDA, 2011; Zhou, 2008). The above data can provide initial information for future DDI studies if drug development using primycin continues. Further evidence that primycin-sulphate can interfere with the lipid metabolism was demonstrated in tissue sections where lipid staining was drastically reduced by primycin-sulphate (Fig. 2I). Modification of the lipid metabolism was also confirmed by Affymetrix gene expression studies where expression of several lipid metabolism associated genes were detected (Di Pietro et al., 2010; Pirat et al., 2017). These consisted of: up-regulation of PDK4 (Kulkarni et al., 2012), a kinase that plays a key role in regulation of glucose and fatty acid metabolism and homeostasis, up-regulation of serine/threonine kinase SGK1 (Pirat et al., 2017) that plays an important role in cellular stress response that activates certain potassium, sodium, and chloride channels. Also, down-regulation of APOB and FABP1 were triggered by primycin-sulphate (Fig. 2E). While FABP1 or LFABP (liver-type fatty acid-binding protein) is responsible for transport and metabolism of long-chain fatty acids (LCFAs), endocannabinoids and other hydrophobic molecules (Schroeder et al., 2016), APOB, is the primary apolipoprotein of LDL – known commonly as "bad cholesterol" (Cromwell and Barringer, 2009; Fisher et al., 2014). Although the indications are clear, further studies are needed to understand the complex effects of primycin-sulphate on human tissues and the consequences of lipid modulation.

In summary, our study provided the first opportunity to assess the effects of primycin-sulphate on the human liver. The 3D co-culture liver model system (Alexandre et al., 1999; Barbier et al., 2003; Choi et al., 2009; Elliott and Yuan, 2011; Gómez-Lechón et al., 2007, 2004; Hewitt and Hewitt, 2004; Houssaint, 1980; Olson et al., 1990; Thomas et al., 2005) was suitable for an initial screening (Bhatia et al., 1999; Riccalton-Banks et al., 2003) of a drug that might be an effective antibiotic even against multiresistant bacterial strains. Our study has shown that even if the solubility issues were to be resolved (Keck and Müller, 2006; Kesisoglou et al., 2007) further studies are certainly needed to develop a primycin-based oral or parenteral preparation.

Acknowledgments

JEP was supported by the European Union and the State of Hungary, co-financed by the European Social Fund in the framework of TÁMOP-4.2.4.A/2-11/1-2012-0001 'National Excellence Program'.

This work was also supported by the GINOP 2.3.2-15-2016-00022 grant. The project has been supported by the European Union, co-financed by the European Regional Development Fund.

The authors (EA, JR, GM, KK, JEP) declare no conflict of interest, while AP, CF, ZP, JBB declared conflict of interest holding a patent or having been financially supported in association with the study.

The authors wish to thank Mr Ricky Odedra for language editing.

Appendix A. Supplementary data

Supplementary data associated with this article can be found, in the online version, at http://dx.doi.org/10.1016/j.toxlet.2017.09.005.

References

Adám-Vizi, V., Horváth, I., Vizi, E.S., 1980. Acetylcholine-releasing effect of primycin, a highly active antibiotic. Pharmacology 20, 268–274.

Alexandre, E., David, P., Viollon, C., Wolf, P., Jaeck, D., Azimzadeh, A., Nicod, L., Boudjema, K., Richert, L., 1999. Expression of cytochromes P-450 2E1, 3A4 and 1A1/1A2 in growing and confluent human HepG2 hepatoma cells-effect of ethanol.

Toxicol. In Vitro 13, 427–435.
Bálint, G., 1987. Favourable observations with Ebrimycin gel in the outpatient department of surgery. Ther. Hung. 35, 140–142.
Bíró, J., Várkonyi, V., 1987. Ebrimycin gel in the treatment of pyodermas and bacterial secondary infections. Ther. Hung. 35, 136–139.
Barbier, O., Duran-Sandoval, D., Pineda-Torra, I., Kosykh, V., Fruchart, J.-C., Staels, B., 2003. Peroxisome proliferator-activated receptor alpha induces hepatic expression of the human bile acid glucuronidating UDP-glucuronosyltransferase 2B4 enzyme. J. Biol. Chem. 278, 32852–32860. http://dx.doi.org/10.1074/jbc.M305361200.
Bell, C.C., Hendriks, D.F.G., Moro, S.M.L., Ellis, E., Walsh, J., Renblom, A., Fredriksson, L., Puigvert Dankers, Jacobs, F., Snoeys, J., Sison-Young, R.L., Jenkins, R.E., 2016. Characterization of primary human hepatocyte spheroids as a model system for drug-induced liver injury, liver function and disease. Sci. Rep. 6.
Bhatia, S.N., Balis, U.J., Yarmush, M.L., Toner, M., 1999. Effect of cell–cell interactions in preservation of cellular phenotype: cocultivation of hepatocytes and nonparenchymal cells. FASEB J. 13, 1883–1900.
Blaskó, K., Shagina, L.V., Gyorgyi, S., Lev, A.A., 1986. The mode of action of some antibiotics on red blood cell membranes. Gen. Physiol. Biophys. 5, 625–635.
Breslin, S., O'Driscoll, L., 2013. Three-dimensional cell culture: the missing link in drug discovery. Drug Discov. Today 18 (5/6), 240–249.
Carls, A., Jedamzik, J., Witt, L., Hohmann, N., Burhenne, J., Mikus, G., 2014. Systemic exposure of topical erythromycin in comparison to oral administration and the effect on cytochrome P450 3A4 activity. Br. J. Clin. Pharmacol. 78, 1433–1440. http://dx.doi.org/10.1111/bcp.12497.
Chavey, C., Fajas, L., 2009. CXCL5 drives obesity to diabetes, and further. Aging (Albany, NY) 1, 674–677. http://dx.doi.org/10.18632/aging.100064.
Choi, S., Sainz, B., Corcoran, P., Uprichard, S., Jeong, H., 2009. Characterization of increased drug metabolism activity in dimethyl sulfoxide (DMSO)-treated Huh7 hepatoma cells. Xenobiotica 39, 205–217. http://dx.doi.org/10.1080/00498250802613620.
Chougule, P., Sumitran-Holgersson, S., Hamilton Dr., G., 2012. Cytokeratins of the Liver and Intestine Epithelial Cells During Development and Disease. Cytokeratins ? Tools in Oncology. InTech ISBN: 978-953-51-0047-8, Available from. http://www.intechopen.com/books/cytokeratins-tools-in-oncology/cytokeratins-of-the-liver-and-intestine-epithelial-cells-during-development-and-disease.
Cromwell, W.C., Barringer, T.A., 2009. Low-density lipoprotein and apolipoprotein B: clinical use in patients with coronary heart disease. Curr. Cardiol. Rep. 11, 468–475.
DeVane, C.L., Donovan, J.L., Liston, H.L., Markowitz, J.S., Cheng, K.T., Risch, S.C., Willard, L., 2004. Comparative CYP3A4 inhibitory effects of venlafaxine, fluoxetine, sertraline, and nefazodone in healthy volunteers. J. Clin. Psychopharmacol. 24, 4–10. http://dx.doi.org/10.1097/01.jcp.0000104908.75206.26.
Di Pietro, N., Panel, V., Hayes, S., Bagattin, A., Meruvu, S., Pandolfi, A., Hugendubler, L., Fejes-Tóth, G., Naray-Fejes-Tóth, A., Mueller, E., 2010. Serum- and glucocorticoid-inducible kinase 1 (SGK1) regulates adipocyte differentiation via forkhead box O1. Mol. Endocrinol. 24, 370–380. http://dx.doi.org/10.1210/me.2009-0265.
Elliott, N.T., Yuan, F., 2011. A review of three-dimensional in vitro tissue models for drug discovery and transport studies. J. Pharm. Sci. 100, 59–74. http://dx.doi.org/10.1002/jps.22257.
Ernest, C.S., Hall, S.D., Jones, D.R., 2004. Mechanism-based inactivation of CYP3A by HIV protease inhibitors. J. Pharmacol. Exp. Ther. 312, 583–591. http://dx.doi.org/10.1124/jpet.104.075416.
FDA, 2011. No Title [WWW Document], Drug Dev. Drug Interact. Table Substrates, Inhib. Inducers.
Feiszt, P., Mestyán, G., Kerényi, M., Dobay, O., Szabó, J., Dombrádi, Z., Urbán, E., Emődy, L., 2014. Re-evaluation of in vitro activity of primycin against prevalent multi-resistant bacteria. Int. J. Med. Microbiol. 304, 1077–1085. http://dx.doi.org/10.1016/j.ijmm.2014.08.001.
Feiszt, P., Schneider, G., Emődy, L., 2017. Effect of primycin on growth-arrested cultures and cell integrity of Staphylococcus aureus. Acta Microbiol. Immunol. Hung. 64, 121–130. http://dx.doi.org/10.1556/030.64.2017.002.
Fisher, E., Lake, E., McLeod, R.S., 2014. Apolipoprotein B100 quality control and the regulation of hepatic very low density lipoprotein secretion. J. Biomed. Res. 28, 178–193. http://dx.doi.org/10.7555/JBR.28.20140019.
Gómez-Lechón, M.J., Donato, M.T., Castell, J.V., Jover, R., 2004. Human hepatocytes in primary culture: the choice to investigate drug metabolism in man. Curr. Drug Metab. 5, 443–462.
Gómez-Lechón, M.J., Castell, J.V., Donato, M.T., 2007. Hepatocytes–the choice to investigate drug metabolism and toxicity in man: in vitro variability as a reflection of in vivo. Chem. Biol. Interact. 168, 30–50. http://dx.doi.org/10.1016/j.cbi.2006.10.013.
Gumerova, A.A., Titova, M.A., Kiassov, A.P., 2007. Expression of different liver cell markers during the early prenatal human development. Cell Tissue Biol. 1, 143–150. http://dx.doi.org/10.1134/S1990519x 07020058.
Hewitt, N.J., Hewitt, P., 2004. Phase I and II enzyme characterization of two sources of HepG2 cell lines. Xenobiotica 34, 243–256. http://dx.doi.org/10.1080/00498250310001657568.
Horváth, I., Kramer, M., Bauer, P.I., Büki, K.G., 1979. The mode of action of primycin. Arch. Microbiol. 121, 135–139.
Houssaint, E., 1980. Differentiation of the mouse hepatic primordium. I. An analysis of tissue interactions in hepatocyte differentiation. Cell Differ. 9, 269–279.
Hu, J.M., Camper, S.A., Tilghman, S.M., Miller, T., Georgoff, I., Serra, R., Isom, H.C., 1992. Functional analyses of albumin expression in a series of hepatocyte cell lines and in primary hepatocytes. Cell Growth Differ. 3, 577–588.
Johnstone, C.N., Chand, A., Putoczki, T.I., Ernst, M., 2015. Emerging roles for IL-11 signaling in cancer development and progression: focus on breast cancer. Cytokine Growth Factor Rev. 26/5, 489–498.
Keck, C.M., Müller, R.H., 2006. Drug nanocrystals of poorly soluble drugs produced by high pressure homogenisation. Eur. J. Pharm. Biopharm. 62, 3–16. http://dx.doi.org/10.1016/j.ejpb.2005.05.009.
Kesisoglou, F., Panmai, S., Wu, Y., 2007. Nanosizing–oral formulation development and biopharmaceutical evaluation. Adv. Drug Deliv. Rev 59, 631–644. http://dx.doi.org/10.1016/j.addr.2007.05.003.
Khetani, S.R., Bhatia, S.N., 2008. 2008. Microscale culture of human liver cells for drug development. Nat. Biotechnol. 26, 120–126. http://dx.doi.org/10.1038/nbt1361.
Kulkarni, S.S., Salehzadeh, F., Fritz, T., Zierath, J.R., Krook, A., Osler, M.E., et al., 2012. Mitochondrial regulators of fatty acid metabolism reflect metabolic dysfunction in type 2 diabetes mellitus. Metabolism 61, 175–185. http://dx.doi.org/10.1016/j.metabol.2011.06.014.
Mészáros, L., König, T., Paróczai, M., Náhm, K., Horváth, I., 1979. Effect of primycin on the inner membrane permeability of rat liver mitochondria. J. Antibiot. (Tokyo) 32, 161–166.
Malinen, M.M., Kanninen, L.K., Corlu, A., Isoniemi, H.M., Lou, Y.-R., Yliperttula, M.L., Urtti, A.O., 2014. Differentiation of liver progenitor cell line to functional organotypic cultures in 3D nanofibrillar cellulose and hyaluronan-gelatin hydrogels. Biomaterials 35, 5110–5121. http://dx.doi.org/10.1016/j.biomaterials.2014.03.020.
Manesh, M.E., Esmaeilzadehb, A., Mirzaeid, M.H., 2015. IL-24: A novel gene therapy candidate for immune system upregulation in Hodgkin's lymphoma. J. Med. Hypotheses Ideas 9/1, 61–66.
Nógrádi, M., 1988. Primycin (Ebrimycin®) – a new topical antibiotic, 24, 563–566.
Olson, M., Mancini, M., Venkatachalam, M., Roy, A., 1990. Hepatocyte Cytodifferentiation and Cell-to-cell Communication. pp. 71–92.
Papp, T., Ménesi, L., Szalai, I., 1990. Experiences in the Ebrimycin gel treatment of burns. Ther. Hung. 38, 125–128.
Pirat, C., Dacquet, C., Leclerc, V., Hennuyer, N., Beucher-Gaudin, M., Zanirato, G., Géant, A., Staels, B., Ktorza, A., Farce, A., Caignard, D.-H., Berthelot, P., Lebegue, N., 2017. Anti-diabetic activity of fused PPARγ-SIRT1 ligands with limited body-weight gain by mimicking calorie restriction and decreasing SGK1 expression. Eur. J. Med. Chem. 137, 310–326. http://dx.doi.org/10.1016/j.ejmech.2017.06.006.
Riccalton-Banks, L., Liew, C., Bhandari, R., Fry, J., Shakesheff, K., 2003. Long-term culture of functional liver tissue: three-dimensional coculture of primary hepatocytes and stellate cells. Tissue Eng. 9, 401–410. http://dx.doi.org/10.1089/107632703322066589.
Schroeder, F., McIntosh, A.L., Martin, G.G., Huang, H., Landrock, D., Chung, S., Landrock, K.K., Dangott, L.J., Li, S., Kaczocha, M., Murphy, E.J., Atshaves, B.P., Kier, A.B., 2016. Fatty acid binding protein-1 (FABP1) and the human FABP1 T94A variant: roles in the endocannabinoid system and dyslipidemias. Lipids 51, 655–676. http://dx.doi.org/10.1007/s11745-016-4155-8.
Sevrioukova, I.F., Poulos, T.L., 2010. Structure and mechanism of the complex between cytochrome P4503A4 and ritonavir. Proc. Natl. Acad. Sci. 107, 18422–18427. http://dx.doi.org/10.1073/pnas.1010693107.
Song, S., Attia, R.R., Connaughton, S., Niesen, M.I., Ness, G.C., Elam, M.B., Hori, R.T., Cook, G.A., Park, E.A., 2010. Peroxisome proliferator activated receptor α (PPARα) and PPAR gamma coactivator (PGC-1α) induce carnitine palmitoyltransferase IA (CPT-1A) via independent gene elements. Mol. Cell. Endocrinol. 325, 54–63. http://dx.doi.org/10.1016/j.mce.2010.05.019.
Straus, D.S., Glass, C.K., 2007. Anti-inflammatory actions of PPAR ligands: new insights on cellular and molecular mechanisms. Trends Immunol. 28, 551–558. http://dx.doi.org/10.1016/j.it.2007.09.003.
Thomas, R.J., Bhandari, R., Barrett, D.A., Bennett, A.J., Fry, J.R., Powe, D., Thomson, B.J., Shakesheff, K.M., 2005. The effect of three-dimensional co-culture of hepatocytes and hepatic stellate cells on key hepatocyte functions in vitro. Cells. Tissues Organs 181, 67–79. http://dx.doi.org/10.1159/000091096.
Uri, J.V., Actor, P., 1979. Crystallization and antifungal activity of primycin. J. Antibiot. (Tokyo) 32, 1207–1209.
Uri, J.V., 1986. Antibacterial activity of primycin against multiple strains of gram-positive bacteria. Acta Microbiol. Hung. 33, 141–146.
Valyi-Nagy, T., Kelentey, B., 1960. The toxicology and pharmacology of primycin. Arch. Int. Pharmacodyn. Thér. 124, 466–481.
Valyi-Nagy, T., Uri, J., Szilagyi, I., 1954. Primycin, a new antibiotic. Nature 174, 1105–1106.
Vermeer, L.M.M., Isringhausen, C.D., Ogilvie, B.W., Buckley, D.B., 2016. Evaluation of ketoconazole and its alternative clinical CYP3A4/5 inhibitors as inhibitors of drug transporters: the In vitro effects of ketoconazole, ritonavir, clarithromycin, and itraconazole on 13 clinically-Relevant drug transporters. Drug Metab. Dispos. 44, 453–459. http://dx.doi.org/10.1124/dmd.115.067744.
Virág, E., Pesti, M.S., Kunsági-Máté, S., 2012. Complex formation between primycin and ergosterol: entropy–driven initiation of modification of the fungal plasma membrane structure. J. Antibiot. (Tokyo) 65, 193–196. http://dx.doi.org/10.1038/ja.2011.140.
Virag, E., Pesti, M., Kunsagi-Mate, S., 2010. Competitive hydrogen bonds associated with the effect of primycin antibiotic on oleic acid as a building block of plasma membranes. J. Antibiot. 63, 113–117.
Zhou, S.-F., 2008. Drugs behave as substrates, inhibitors and inducers of human cytochrome P450 3A4. Curr. Drug Metab. 9, 310–322.